NMR Solution Structure of Phospholamban

by **Stefanie Lamberth**[a]), **Holger Schmid**[b]), **Martin Muenchbach**[b]), **Thomas Vorherr**[b]), **Joachim Krebs**[b]), **Ernesto Carafoli**[b])[c]), and **Christian Griesinger***[a])[1])

[a]) Institute of Organic Chemistry, University of Frankfurt, Marie-Curie-Str. 11, D-60439 Frankfurt (Phone: +49 69 79829130; fax: +49 69 79829128; e-mail: cigr@org.chemie.uni-frankfurt.de)

[b]) Institute of Biochemistry, Swiss Federal Institute of Technology (ETH), Universitätstrasse 16, CH-8092 Zürich

[c]) Department of Biological Chemistry, University of Padova, Via Colombo, I-35121 Padova

Dedicated to Professor *Albert Eschenmoser* on the occasion of his 75th birthday

Phospholamban (PLN), an amphipathic intrinsic membrane protein of 52 amino acids, is the modulator of the Ca^{2+} pump of cardiac, slow-twitch, and smooth-muscle sarcoplasmic reticulum. In response to β-adrenergic stimulation, it becomes phosphorylated at Ser^{16} and/or Thr^{17}, and dissociates from the pump, which, in turn, achieves its full activity. Here we present the three-dimensional structure of chemically synthesized, monomeric PLN in an organic solvent. Monomerization (PLN normally forms homopentamers) was obtained by replacing Cys^{41} with phenylalanine (Phe = F), a modification that did not affect biological activity. The structure was determined by high-resolution NMR in $CHCl_3$/MeOH of the unphosphorylated state of [F^{41}]PLN (C41F). Of the hydrophilic cytoplasmic parts IA (Met^1 to Pro^{21}) and IB (Gln^{22} to Asn^{30}) and the membrane-spanning hydrophobic domain II (Leu^{31} to Leu^{52}) of PLN, domain IA, which contains the two phosphorylation sites Ser^{16} and Thr^{17}, and domain II have been suggested to be helical and connected through the less-structured hinge-region IB. In the structural study presented here, [F^{41}]PLN is composed of two α-helical regions connected by a β-turn (type III). The residues of the β-turn (type III) are Thr^{17}, Ile^{18}, Glu^{19}, and Met^{20}, the first being one of the two phosphorylation sites (Ser^{16} and Thr^{17}). The hinge region is located at the C-terminal end of domain IA, and domain IB is part of a second helix. The two α-helices comprising amino acids 4 – 16 and 21 – 49 are well-defined (the root-mean-square deviations for the backbone atoms, calculated for a family of the structures, are 0.58 and 0.92 Å, resp.). Pro^{21} is at the beginning of the C-terminal helix and in the *trans* conformation.

Introduction. – Free Ca^{2+} in the myoplasm controls the contraction and relaxation of muscles. The sarcoplasmic reticulum (SR) calcium pump (SERCA), a 110 kDa protein belonging to the family of P-type ATPases [1] removes Ca^{2+} from the myoplasm and works in association with Ca^{2+}-releasing channels in the SR membrane to maintain the appropriate calcium level in the cell. In cardiac muscles, the activity of the Ca^{2+} pump is modulated by β-adrenergic agonists, which regulate contractile force and muscle relaxation [2]. These effects are mediated by the phosphorylation of a small amphipathic SR protein, phospholamban (PLN), by two kinases [3][4]. PLN is a membrane-intrinsic protein of 52 amino acids (see *Fig. 1*) that interacts with the cardiac, slow-twitch, and smooth-muscle isoforms of the SERCA pump, keeping it in an inhibited state. Phosphorylation of PLN Ser^{16} by the cAMP-dependent protein kinase (PKA) [4] or of Thr^{17} by a calmodulin-dependent kinase [5], or of both, causes PLN dissociation from the ATPase, relieving its inhibition.

---

[1]) Also: Max Planck Institut für biophysikalische Chemie, Am Faßberg, D-37077 Göttingen, Germany.

Fig. 1. *Amino acid sequence of PLN.* The two phosphorylation sites Ser[16] and Thr[17] are underlined, and the position of the mutation (replacement of Cys[41] by Phe[41] yielding [F[41]]PLN) is doubly underlined.

Cross-linking experiments by *James et al.* [6] using a photoaffinity labeling probe showed that Lys[3] of PLN in the cytoplasmic domain bound to a region of the Ca^{2+} pump just downstream of its phosphorylation site (Asp[351]). The efficiency of cross-linking was significantly reduced by calcium or when PLN was phosphorylated. These results indicated that PLN inhibits the pump through electrostatic interactions involving basic residues in the N-terminal, cytosolic domain of PLN and acidic residues near the active site of the pump, *i.e.*, the ATP-binding site and the phosphorylated aspartate. This view was corroborated by mutagenesis experiments [7], which confirmed that residues 397–402 ([397]DDKPV[402]), in the acylphosphorylation domain of the pump were critical for the interaction, stressing the importance of charged side chains in the interaction of the two proteins. On the other hand, recent mutational screening experiments [8][9] have provided evidence for hydrophobic interactions between the transmembrane domains of PLN (domain II) and of the Ca^{2+} pump, especially transmembrane helix 6 of the latter.

PLN has a strong tendency to form homopentamers. However, according to recent evidence (see below), the form that regulates the SERCA pump *in vivo* is the monomer [10]. It was thus decided to determine the structure of monomeric PLN, specifically, that of the [F[41]]PLN monomer (replacement of Cys[41] by Phe[41]), which has no propensity to form pentamers and the biological activity of which is similar to that of wild-type PLN [11]. Structural studies on portions of PLN have provided evidence for a high helical content of the protein [12][13], in agreement with preliminary NMR experiments on the PLN mutant [F[41]]PLN (also called C41F) [14]. The work presented here describes the first determination of the three-dimensional structure of [F[41]]PLN, obtained by two-dimensional homonuclear NMR spectroscopy. It shows that [F[41]]PLN is composed of two helical portions spanning residues 4–16 (adjacent to the kinase substrates Ser[16] and Thr[17]) and 21–49. The two helices are connected by a β-turn (type III) that includes one of the phosphorylation sites, Thr[17].

Results and Discussion. – *NMR-Spectroscopy and Assignment of [41-Phenylalanine]phospholamban* ([F[41]]PLN). The structure of [F[41]]PLN was determined by two-dimensional homonuclear NMR spectroscopy in $CHCl_3$/MeOH 1:1 (*v*/*v*), a solvent mixture mimicking the environment of biological membranes [15]. The ^{1}H-NMR assignments of the majority of amino-acid spin systems were obtained by a combination of DQF-COSY and TOCSY experiments conducted according to standard procedures [16]. Because of missing cross-peaks in the H^N,H^α region of the DQF-COSY due to small $^3J_{HNH\alpha}$ coupling constants or overlap of the cross-peaks, a TOCSY with a mixing time of 30 ms was used to identify those cross-peaks. At an early stage of the assignment, the unique amino acids Asp[2], Lys[3], Tyr[6], and Pro[21] were assigned unambiguously. In the case of Asp[2], Lys[3], and Pro[21], the typical spin systems of the amino acids were detected in the DQF-COSY, and in the case of Tyr[6] the resonances of the aromatic side chain could be easily recognized in the 800-MHz NOESY. Most of the other spin systems could be identified, but for the sequential assignment, the 800-MHz

NOESY proved indispensible (*Fig. 2*). Except for Ser[10], Arg[14], Met[20], Cys[36], and Ile[47], all spin systems could be determined by analyzing the sequential H^{α},HN(i,$i+1$) and H^N,H^N(i,$i+1$) cross-peaks. For the above-mentioned five amino acids, the assignment was accomplished by means of the medium-range H^{α},H^N(i,$i+3$) and H^{α},H^N(i,$i+4$) cross-peaks in the 800-MHz NOESY (*Fig. 3*). The assignments are listed in *Table 1*.

Only five $^3J_{HNH\alpha}$ coupling constants could be measured from the fine structure of COSY cross-peaks by comparison with the in-phase *m*s of cross-peaks in the NOESY [17]. In this region of the spectra, several cross-peaks were missing due to small coupling constants (<4 Hz) or overlap of the cross-peaks.

The H^{α} chemical shifts of the residues Val[4] to Thr[17] and Gln[23] to Val[49] are shifted to higher field compared to their random-coil values, implying an α-helical structure

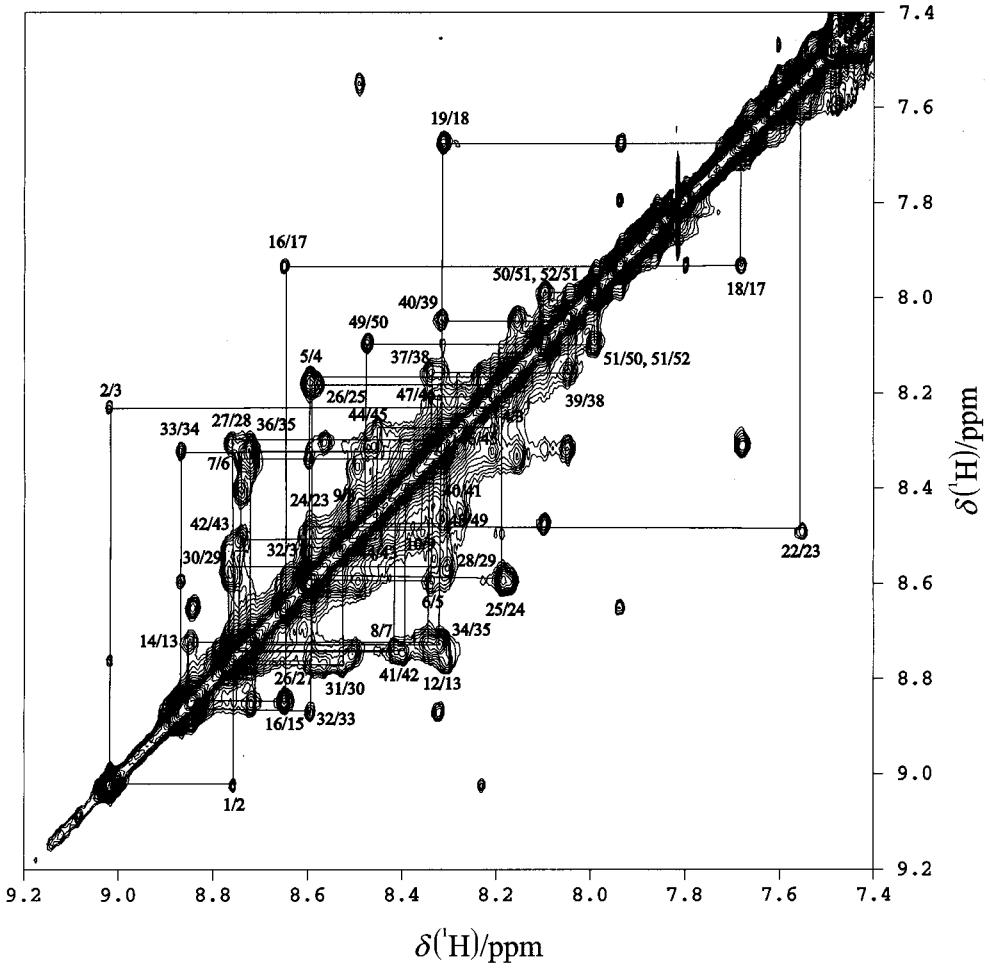

Fig. 2. *H^N,H^N Region of the 800-MHz NOESY, acquired at 300 K with a mixing time of 150 ms, of 1 mM [F^{41}]PLN in $CHCl_3$/MeOH 1:1 (v/v)*. Sequential NOEs are indicated in the spectrum, the first number refers to the H^N resonance in ω_1, the second to that in ω_2.

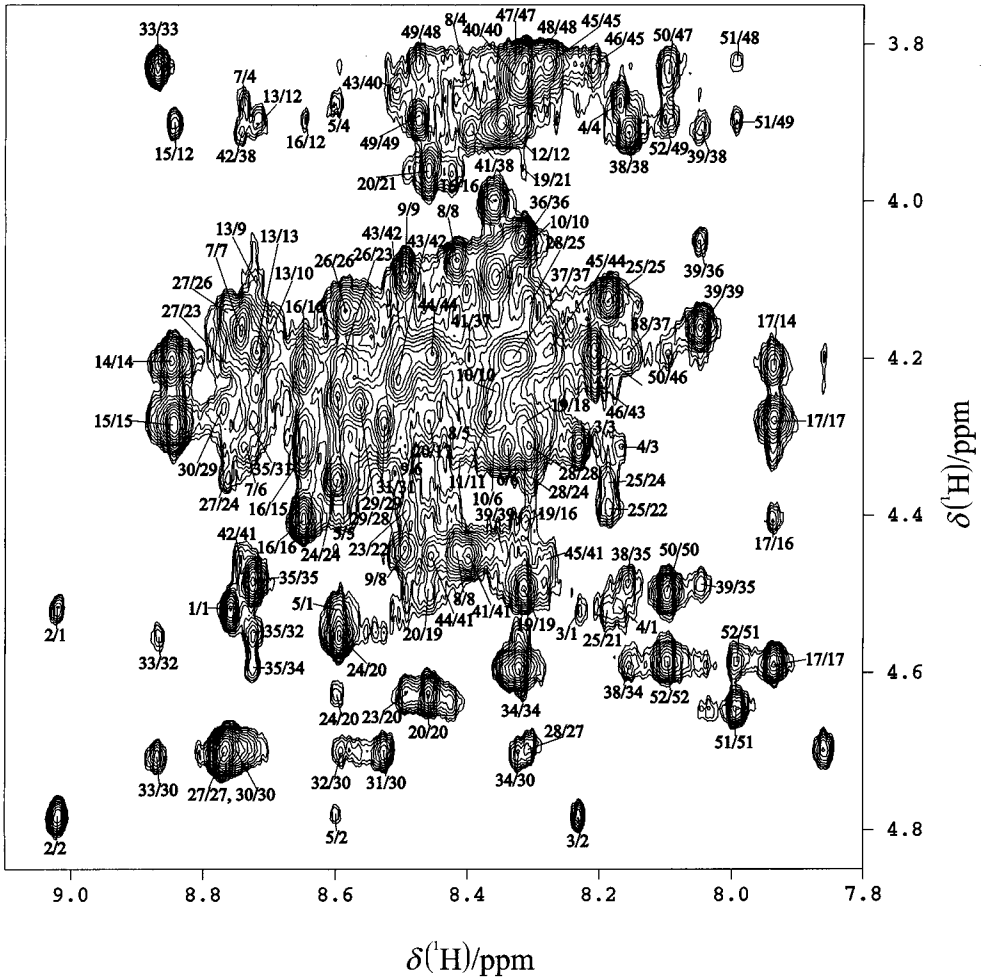

Fig. 3. *Fingerprint region of the 800-MHz NOESY, acquired at 300 K with a mixing time of 150 ms, of 1 mM [F*^{41}*]PLN* in *$CHCl_3$/MeOH 1:1 (v/v)*. Assigned cross-peaks are indicated in the spectrum, the first number refers to the H^{α} resonance in ω_1, the second to the H^N resonance in ω_2.

(*Fig. 4,a*) [18]. However, as discussed in detail below, Thr^{17} is part of a β-turn (type III) between the two helical portions. The H^{α} resonances of Ile^{18}, Glu^{19}, and Pro^{21}, and of the residues at the carboxy terminus, on the other hand, are at low field compared to their random-coil values. Met^1 and Asp^2 at the amino terminus and Met^{20} show only a small chemical-shift deviation from the random-coil value.

The 800-MHz NOESY experiment was used to identify 644 NOE restraints (398 intraresidual, 142 sequential, and 104 medium-range) within [F^{41}]PLN (*Fig. 4,b*), corresponding to an average of 12.4 NOEs per residue. *Fig. 5* shows the number of NOE restraints per residue. NOEs that range longer than from residues i to $i+4$ were not observed.

Table 1. *[41-Phenylalanine]phospholamban [F41]PLN ^{1}H-NMR Assignment* ($CDCl_3/CD_3OH$ (1:1 (*v/v*))

Residue	H^N	H^α	H^β	Others
Met 1	8.76	4.45	2.22 (*pro-S*), 2.28 (*pro-R*)	H^γ 2.83 (*pro-S*), 2.77 (*pro-R*)
Asp 2	9.02	4.68	3.16 (*pro-R*), 3.03 (*pro-S*)	
Lys 3	8.10	4.24	2.08 (*pro-R*), 2.21 (*pro-S*)	H^γ 1.82 (*pro-R*), 1.68 (*pro-S*), H^δ 1.89, H^ε 3.12
Val 4	8.08	3.82	2.42	H^γ 1.28 (*pro-R*), 1.16 (*pro-S*)
Gln 5	8.53	4.20	2.43	H^γ 2.67 (*pro-R*), 2.54 (*pro-S*), H^ε 7.55, 6.75
Tyr 6	8.28	4.27	3.31	H^δ 7.17, H^ε 6.89
Leu 7	8.66	4.10	2.12 (*pro-S*), 1.79 (*pro-R*)	H^δ 1.15
Thr 8	8.36	4.02	4.39	H^γ 1.41
Arg 9	8.44	4.15	1.99 (*pro-S*), 2.15 (*pro-R*)	H^γ 1.80, H^δ 3.36, H^ε 7.78
Ser 10	8.30	4.20	4.05 (*pro-S*), 3.96 (*pro-R*)	
Ala 11	8.31	4.21	1.76	
Ile 12	8.28	3.85	2.12	H^γ 1.74, H^δ 1.03
Arg 13	8.66	4.10	2.13	H^γ 2.08 (*pro-R*), 1.78 (*pro-S*), H^δ 3.37 (*pro-S*), 3.29 (*pro-R*), H^ε 7.81
Arg 14	8.79	4.16	2.14	H^γ 2.05 (*pro-S*), 1.85 (*pro-R*), H^δ 3.34, H^ε 7.52
Ala 15	8.78	4.23	1.74	
Ser 16	8.59	4.36	4.26 (*pro-S*), 4.16 (*pro-R*)	
Thr 17	7.88	4.22	4.53	H^γ 1.52
Ile 18	7.62	4.24	2.18	$H^{\gamma1}$ 1.88, $H^{\gamma2}$ 1.15, H^δ 1.46
Glu 19	8.24	4.44	2.38 (*pro-S*), 2.31 (*pro-R*)	H^γ 2.73, 2.64
Met 20	8.40	4.58	2.56 (*pro-R*), 2.34 (*pro-S*)	H^γ 2.97 (*pro-S*), 2.79 (*pro-R*)
Pro 21		4.47	2.49 (*pro-S*), 2.04 (*pro-R*)	H^γ 2.45 (*pro-R*), 2.15 (*pro-S*), H^δ 3.91
Gln 22	7.51	4.34	2.41 (*pro-R*), 2.35 (*pro-S*)	H^γ 2.66 (*pro-R*), 2.61 (*pro-S*), H^ε 7.75, 6.86
Gln 23	8.43	4.16	2.43 (*pro-R*), 2.34 (*pro-S*)	H^γ 2.55, H^ε 7.46, 6.66
Ala 24	8.53	4.30	1.70	
Arg 25	8.12	4.07	2.21 (*pro-S*), 2.14 (*pro-R*)	H^γ 1.93 (*pro-S*), 1.83 (*pro-R*), H^δ 3.44
Gln 26	8.53	4.10	2.35 (*pro-S*), 2.29 (*pro-R*)	H^γ 2.54 (*pro-S*), 2.42 (*pro-R*), H^ε 7.26, 6.83
Asn 27	8.70	4.64	3.22 (*pro-R*), 2.88 (*pro-S*)	H^δ 7.61, 6.95
Leu 28	8.25	4.25	2.04 (*pro-R*), 1.88 (*pro-S*)	H^δ 1.09
Gln 29	8.51	4.21	2.45 (*pro-R*), 2.35 (*pro-S*)	H^γ 2.64 (*pro-R*), 2.53 (*pro-S*), H^ε 7.49, 6.76
Asn 30	8.71	4.65	3.25 (*pro-R*), 2.95 (*pro-S*)	H^δ 7.79, 6.84
Leu 31	8.48	4.70	2.20 (*pro-S*), 2.11 (*pro-R*)	H^γ 1.93, H^δ 1.09
Phe 32	8.37	4.50	3.49	H^δ 7.40
Ile 33	8.81	3.78	2.26	H^γ 2.14, 1.54, H^δ 1.15
Asn 34	8.27	4.54	3.11 (*pro-R*), 2.84 (*pro-S*)	H^δ 7.41, 6.66
Phe 35	8.67	4.43	3.45	H^δ 7.36
Cys 36	8.26	4.00	3.31 (*pro-R*), 2.76 (*pro-S*)	
Leu 37	8.20	4.14	2.16	H^γ 1.85, H^δ 1.08 (*pro-S*), 1.00 (*pro-R*)
Ile 38	8.11	3.86	2.17	H^γ 1.29, H^δ 1.03
Leu 39	7.91	4.11	1.87	H^γ 1.72, H^δ 0.95
Ile 40	8.26	3.79	2.20	$H^{\gamma1}$ 1.97, $H^{\gamma2}$ 1.32, H^δ 1.00
Phe 41	8.34	4.40	3.25	H^δ 7.39
Leu 42	8.60	4.12	2.15	H^γ 1.73, H^δ 1.07
Leu 43	8.44	4.05	2.07, 1.61	H^δ 1.11
Leu 44	8.36	4.15	2.05	H^γ 1.86, H^δ 1.04
Ile 45	8.23	3.78	2.21	$H^{\gamma1}$ 1.57 (*pro-R*), 1.23 (*pro-S*), $H^{\gamma2}$ 1.07, H^δ 0.79
Cys 46	8.15	4.14	3.46 (*pro-R*), 2.94 (*pro-S*)	
Ile 47	8.25	3.78	2.16	$H^{\gamma1}$ 2.33, 2.20, $H^{\gamma2}$ 1.30, H^δ 1.24
Ile 48	8.47	3.84	2.08	$H^{\gamma1}$ 2.01, $H^{\gamma2}$ 1.30, H^δ 1.02
Val 49	8.32	3.85	2.38	H^γ 1.24 (*pro-R*), 1.14 (*pro-S*)
Met 50	8.02	4.44	2.57 (*pro-S*), 2.32 (*pro-R*)	H^γ 2.96 (*pro-S*), 2.77 (*pro-R*)
Leu 51	7.84	4.59	2.06, 1.77	H^δ 1.06
Leu 52	8.02	4.53	2.08	H^γ 1.76, H^δ 1.04

a)

b)

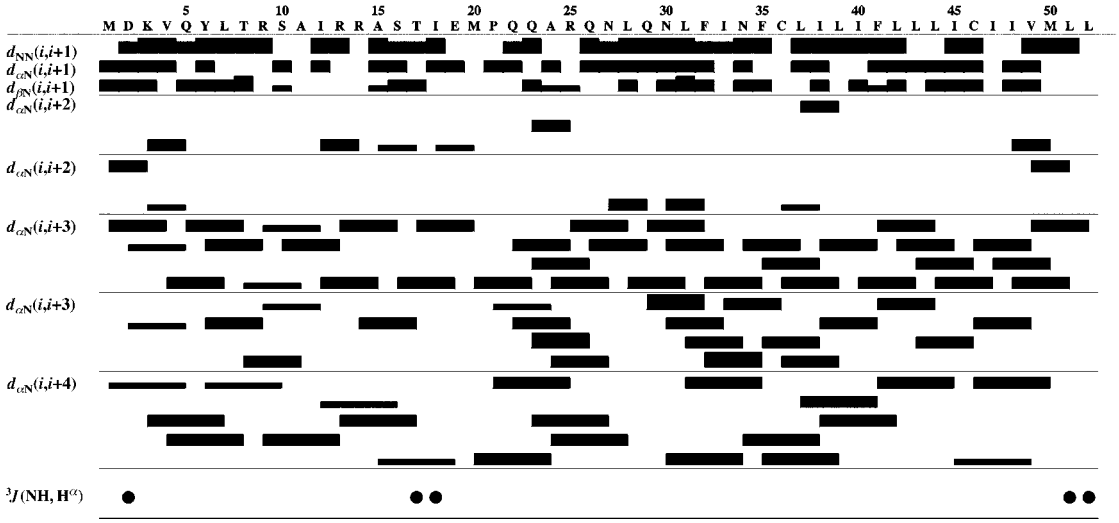

Fig. 4. a) *CSI Plot of the protons H^α according to* [17]. b) *Summary of sequential and medium-range NOEs involving the protons H^N, H^α, and H^β of modified phospholamban [F^{41}]PLN.* Sequential and medium-range NOEs classified as strong, medium, and weak according to the intensity of the cross-peaks are indicated by different heights of the connecting box, ^3J(HN,H^α) are represented by full circles.

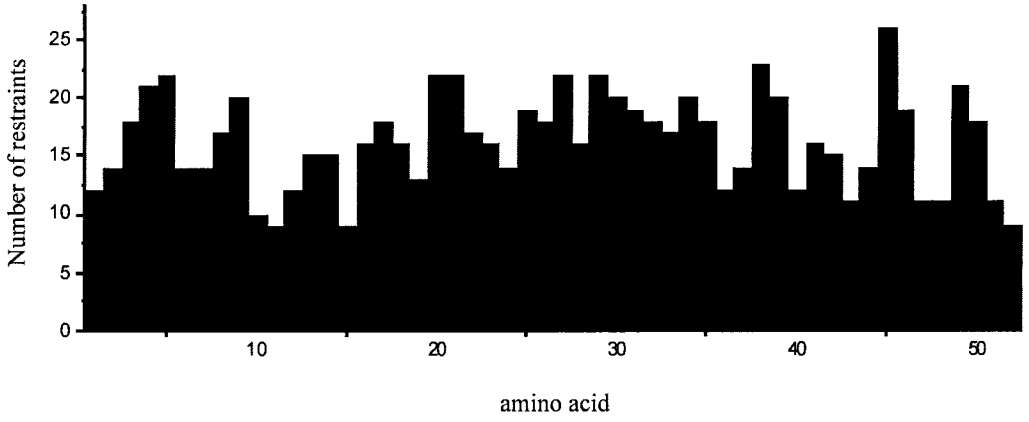

Fig. 5. *Number of NOE restraints per residue*

Structure of [41-Phenylalanine]phospholamban ([F^{41}]PLN). The structural restraints listed were used in a simulated annealing protocol [19] in the program X-PLOR [20] (for details, see *Exper. Part*) to calculate a final set of ten structures. Due to the flexibility of the region between the N- and C-terminal α-helices, it is impossible to superimpose the whole molecule. *Fig. 6* illustrates a best-fit superposition of the backbone atoms of the N-terminal α-helix and of the C-terminal α-helix. The residues at the beginning and at the end of the helical parts are ill-defined by the NMR data and appear disordered. The final ten structures are converged with an r.m.s.d. from the

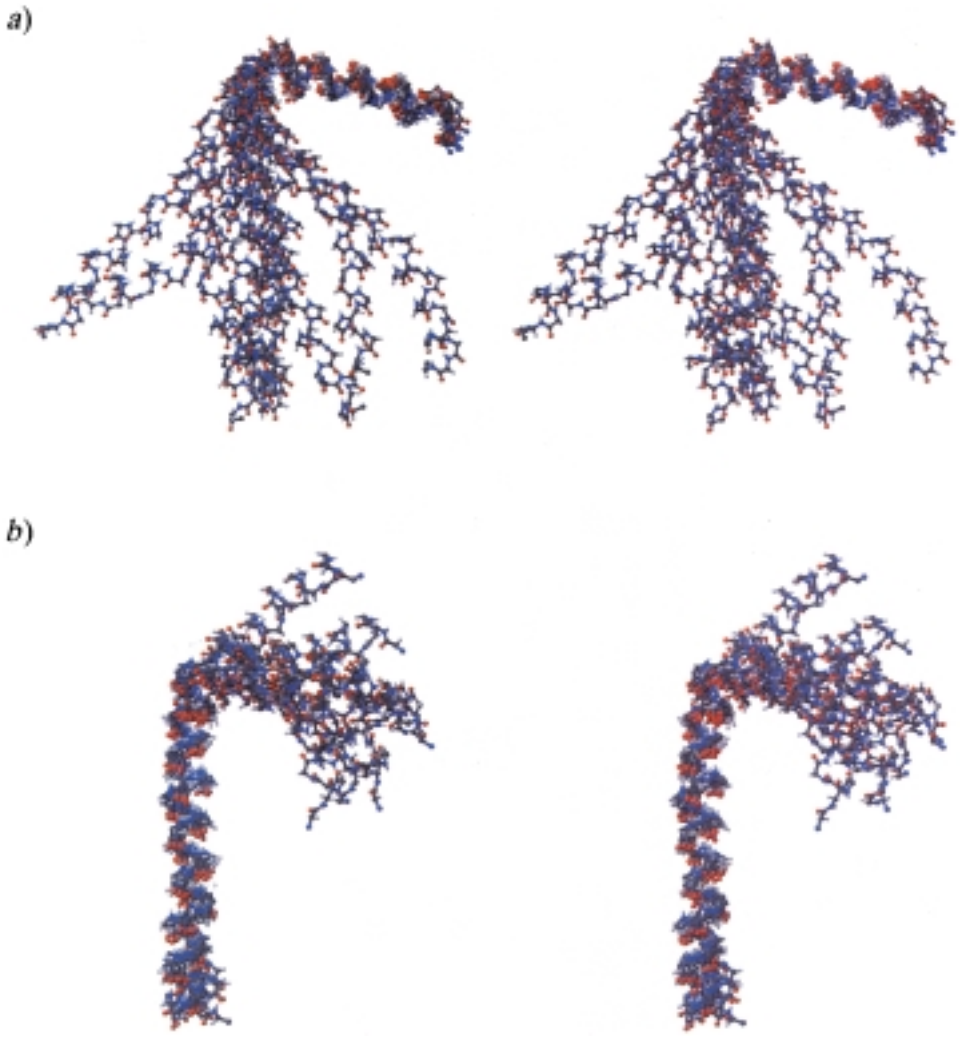

Fig. 6. *Best-fit superpositions of the backbone atoms of* a) *N-terminal helix* (residues Val^4 to Ser^{16}). b) *C-terminal helix* (residues Pro^{21} to Val^{49}) *of the final ten NMR-derived structures of [F^{41}]PLN*. For the N-terminal helix (Val^4 to Ser^{16}), superposition yields an r.m.s.d. value of 0.58 Å and for the C-terminal helix (Pro^{21} to Val^{49}) an r.m.s.d. value of 0.92 Å for all backbone atoms referring to a mean structure.

mean structure of 0.58 Å for all backbone atoms in the N-terminal helix of [F[41]]PLN (residues 4–16) and 0.92 Å for all backbone atoms in the C-terminal helix of [F[41]]PLN (residues 21–49). The ten structures exhibited no distance violations exceding 0.30 Å or dihedral-angle violations exceeding 5° and have an average 89.6% of all residues in the most favorable region of the *Ramachandran* plot according to the PROCHECK-NMR [21] procedure. None of the residues were found in disallowed regions of the *Ramachandran* plot (*Fig. 7*). The structural statistics are summarized in *Table 2*.

The structure of [F[41]]PLN contains two α-helical regions connected by a β-turn (type III) comprising the four residues N-terminal to Pro[21] (*Fig. 8*). These four residues (Thr[17], Ile[18], Glu[19], and Met[20]) have about as many restraints per residue as there were for the residues in the α-helical regions. The mutual orientation of the helices was only weakly restrained by medium-range distance NOEs in the turn. The δ-protons of Pro[21] show only weak NOEs to the H^{α} of Thr[17] and Ile[18] and to the H^{N} of Glu[19]. Therefore, the relative orientation between the two α-helical parts of the molecule is not well-defined.

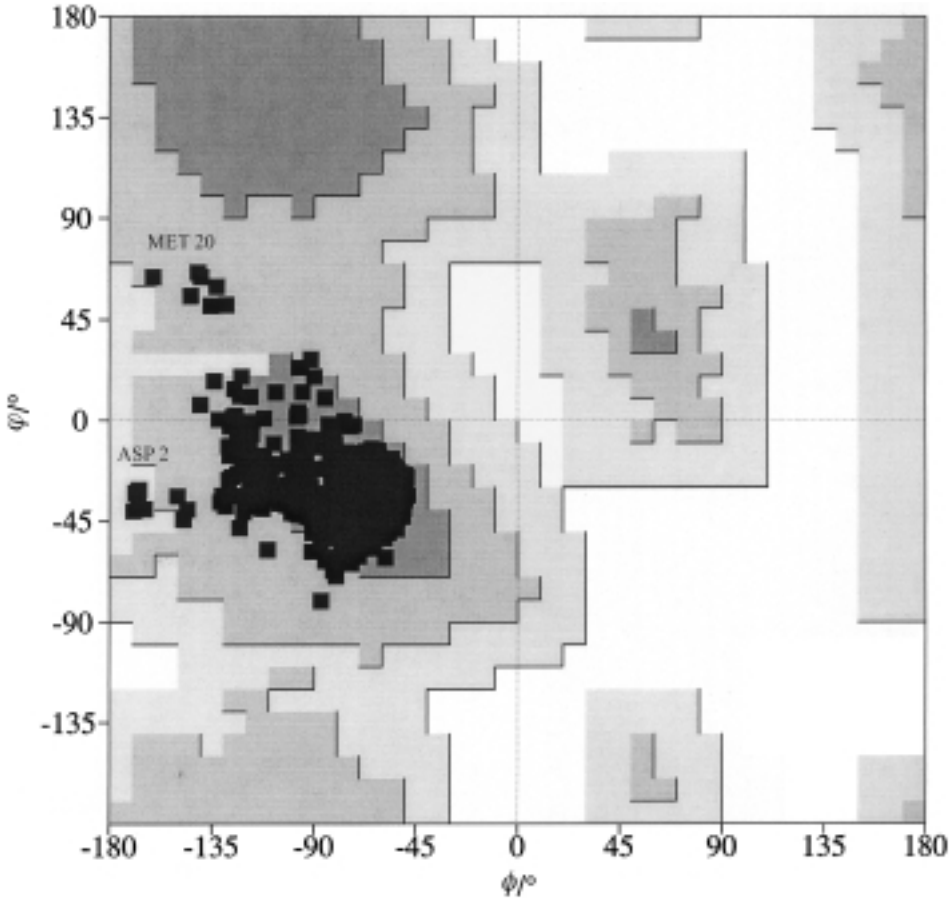

Fig. 7. Ramachandran *plot of the ten final NMR-derived structures of [F[41]]PLN: 90% in the allowed region, 10% in the favored region, and 0% in the disallowed region*

Table 2. *Characteristics of the Structure of [F[41]]PLN in $CDCl_3/CD_3OD$ 1:1 (v/v)*

Parameter	Value
Distance restraints: total	644
intraresidual	398
sequential	142
medium-range	104
Dihedral restraints	5
R.m.s.d. [Å] for region 4–16: backbone atoms	0.58 ± 0.22
heavy atoms	1.51 ± 0.41
R.m.s.d. [Å] for region 21–49: backbone atoms	0.92 ± 0.31
heavy atoms	1.42 ± 0.56
ϕ and ψ in core or allowed	99%

Owing to the structural imprecision in the turn, the family of structures displays a dispersion in the relative position of the amino- and carboxy-terminal helices. But this dispersion is limited, and the interhelical angle is *ca.* $68 \pm 23°$ for ten structures, in agreement with the observation by *Pollesello et al.* [12].

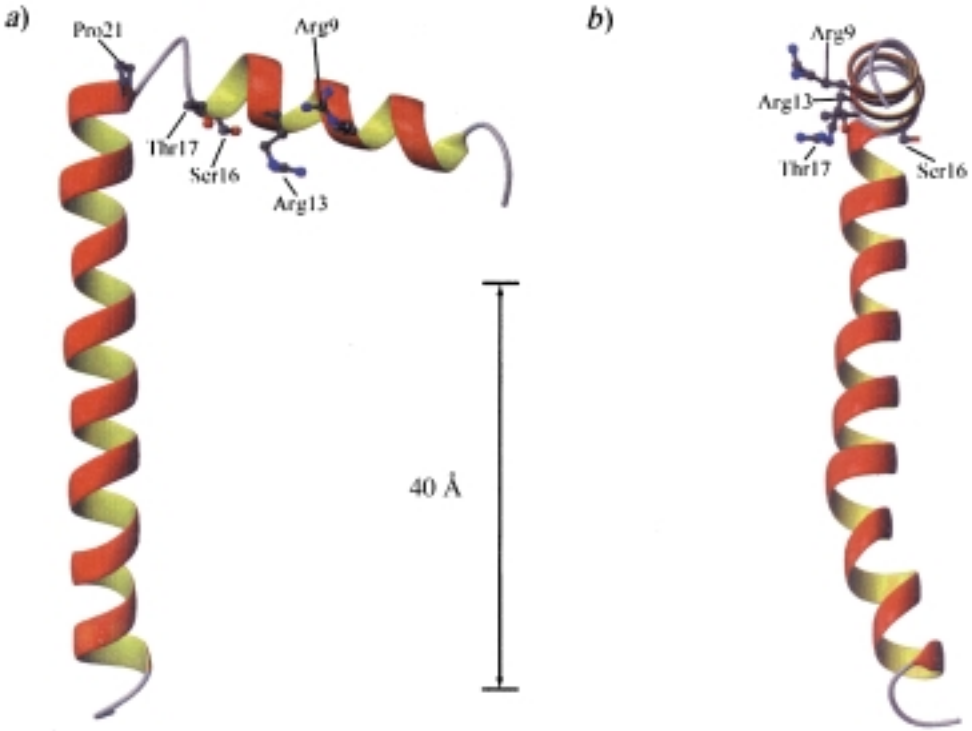

Fig. 8. *Ribbon representation of lowest-energy structure of [F[41]]PLN.* Arg^9, Arg^{13}, Ser^{16}, Thr^{17}, and Pro^{21} side chains are shown. In *b*), the orientation of the side chains Arg^9, Arg^{13}, Ser^{16}, and Thr^{17} are shown. They point towards the C-terminus with a rotation by *ca.* 60° around the N-terminal helix axis. The arrow indicates the postulated transmembrane part of the structure, its length of 40 Å corresponds to the thickness of a lipid bilayer.

Pro[21] does not break the helix as it is actually at the beginning of the C-terminal α-helix. The two phosphorylation sites Ser[16] and Thr[17] are located inside the angle between the two helical regions and face the C-terminal helix. After phosphorylation, the structural arrangement could change and the orientation of the N-terminal helix could differ from that of C-terminal helix as a result of the insertion of the charged phosphate group at Ser[16] and/or Thr[17].

Structure of Phospholamban and its Biochemical Implications. The three-dimensional structure of [F[41]]PLN described here has been obtained for the monomeric form of PLN, which retains full biological activity [11]. The question of whether the active form of PLN in the membrane is a pentamer or a monomer is still controversial. However, recent observations indicate that the form that binds to and inhibits the SERCA pump in the membrane is the monomer rather than the pentamer [22]. This prompted our decision to solve the three-dimensional structure of PLN in its monomeric form to obtain information on its biological function.

Mutagenesis experiments in different laboratories have provided detailed information on the domains of PLN and the SERCA pump involved in the interaction of the two proteins. Recently, *MacLennan* and co-workers [8] have shown that replacing the hydrophobic residues on one face of the transmembrane helix of PLN with alanines reduced the ability of PLN to interact with the pump. Later on, the same group [9] has provided evidence that all SERCA pump residues essential for the interaction are located on one face of its transmembrane helix 6 (M6).

The cross-linking experiments by *James et al.* [6] have suggested an electrostatic interaction between charged residues in the cytosolic domain of PLN and polar residues of the SERCA pump, downstream of Asp[351]. Later experiments by *MacLennan* and co-workers [7] have shown that charged residues in a loop region between Asp[351] and the ATP-binding domain (*i.e.*, [397]DDKPV[402]) of the pump, were critical for its functional interaction with the N-terminal portion of PLN [7]. This was corroborated by the finding by *Hughes et al.* [23] that the positively charged arginines of the N-terminal part of PLN (especially Arg[9] and Arg[13]) were involved in the association with the SERCA pump: in the structure presented here, Arg[9] and Arg[13] lie on the same site of the N-terminal helix as Thr[17]. This was also observed by *Pollesello et al.* [12] on a fragment of PLN (residues 1–36) in a H_2O/CF_3CH_2OH mixture. It appears from the biochemical studies that, to interact with the critical loop region of the SERCA pump, PLN may have to assume a more extended conformation with the helical axes oriented almost parallel to each other. Such a reorientation of the two helices appears possible: When the backbone atoms of the C-terminal helix are superimposed, the N-terminal helix is dispersed in a cone with an opening of almost 90° (*Fig. 6*,*b*). Thus, the potentially required flexibility of PLN around the central hinge region is indeed observed, which may be critical for the ability of the molecule to inhibit the ATPase through the interaction between essential polar residues. Clearly, it will now be important to investigate the structural consequences of the phosphorylation of Ser[16] and/or Thr[17] on the cytosolic region of PLN. It will also be important to perform structural studies on the interaction of PLN with peptides corresponding to the regions of the SERCA pump that are involved in the interaction with PLN. Experiments on these issues are in progress in our laboratories.

This work was supported by the *Fond der chemischen Industrie*, the *DFG*, the *MPG*, the *Graduiertenkolleg: Chemische und Biologische Synthese von Wirkstoffen* (Grk 34/3), and the *VW Foundation*, as well as the *Swiss National Science Foundation* (31-46′998.96), by the *Italian Ministery of University and Scientific Research* (MURST-PRIN, 1998), by the target protein on Biotechnology of the *National Research Council of Italy,* by the *Armenise-Harvard Foundation*, and by the *International Human Frontier Science Program Organization.* All measurements have been performed at the large-scale facility for biomolecular NMR at the University of Frankfurt (ERB CT 950034).

Experimental Part

Sample Preparation. The PLN mutant [F^{41}]PLN (C41F) was synthesized and purified as described by *Vorherr et al.* [24]. The synthesis was accomplished by double couplings and efficient capping procedures. The crude peptide was purified by HPLC ion exchange and gel-permeation chromatography ($CHCl_3$/MeOH). The NMR sample was prepared by solubilizing 6 mg of [F^{41}]PLN in $CDCl_3$/CD_3OH 1:1 (*v*/*v*). The solvents used were CD_3OH (99.8%) and $CDCl_3$ (99.96%). After sonification and centrifugation, the soln. was transferred into a 5-mm NMR tube.

NMR Spectroscopy. All spectra were recorded at a temp. of 300 K using *Bruker-DRX600* and *-DRX800* spectrometers equipped with a *Z*-gradient probe. DQF-COSY [25], TOCSY [26] with mixing times of 30, 50, and 70 ms, and NOESY [27] with mixing times of 100 and 150 ms, were recorded using *States*-TPPI phase cycling [28] for quadrature detection. Relaxation delays of 1–2 s were used (for details, see *Table 3*). Solvent signals were suppressed with selective presaturation or by a gradient echo sequence (WATERGATE) [29]. All data were processed with UXNMR (*Bruker Instruments*, Rheinstetten, Germany) including zero-filling and weighting the indirect dimension with a squared-sine bell function. The spectra were analyzed with FELIX, version 98 (*MSI*, San Diego, CA). Chemical shifts were reported with respect to the signal of the OH group of MeOH at 4.9 ppm.

Table 3. *Acquisition and Processing Parameters for NMR Experiments*

Experiment	Dimension	Acquisition points (complex)	Spectral width [Hz]	Number of scans	Matrix dimension (real points)	Spectrometer
DQF-COSY	*t*1	768	8802	32	1024	*DRX 800*
	*t*2	4096	8803		8192	
TOCSY (30 ms mixing time)	*t*1	768	6601	48	1024	*DRX 600*
	*t*2	4096	6614		4096	
TOCSY (50 ms mixing time)	*t*1	768	6601	40	1024	*DRX 600*
	*t*2	4096	6614		4096	
TOCSY (70 ms mixing time)	*t*1	768	7201	48	1024	*DRX 600*
	*t*2	4096	7184		4096	
NOESY (100 ms mixing time)	*t*1	768	7201	32	1024	*DRX 600*
	*t*2	4096	7184		8192	
NOESY (150 ms mixing time)	*t*1	876	8803	32	1024	*DRX 800*
	*t*2	4096	8803		8192	

Structure Calculations. Distance restraints were determined from the cross-peak intensity by calibration against known interproton distances of geminal protons and classified on the basis of peak intensity with upper bounds of 2.8 Å (strong), 4.0 Å (medium), and 5.0 Å (weak). A correction of 0.5 Å was added to the upper bounds of restraints involving pseudoatoms for Me, CH_2, and aromatic groups [30]. For the lower bounds of the distance restraints, the sum of the *van der Waals* radii was used. The interresidual restraints were treated in the same way as the intraresidual ones. $^3J_{HNH\alpha}$ coupling constants were measured by the method described by *Titman* and *Keeler* [17] from the fine structure of resolved COSY cross-peaks by comparison with the in-phase *m*s of cross-peaks observed in the NOESY and calibrated by the *Karplus* equation [31]. No backbone H-bonds were included in the structure calculations.

All calculations were performed with the X-PLOR program, version 98.1, by *Brünger* [20]. The *ab initio* simulated annealing protocol started with a 32.5 ps high-temperature phase at 2000 K, followed by a first cooling phase of 25 ps, where the temperature was lowered to 1000 K in steps of 50 K. In the second cooling phase, the

temp. was lowered to 100 K, followed by a final energy minimization. A total of 644 NOE-derived distance restraints were applied with a square-well potential and a force constant of 50 kcal · mol^{-1} · Å^{-2}. Restraints involving not stereospecifically assigned CH_2 protons and diastereotopic Me groups of Val and Leu were treated with the floating assignment procedure of X-PLOR. A total of five dihedral-angle restraints from ^3J(HN,H$^\alpha$) coupling constants were also applied with a force constant of 200 kcal · mol^{-1} · rad^{-1}. The final ten structures with the lowest energy were used for the structural statistics. This ensemble of ten structures satisfied the criteria of no NOE violations >0.30 Å and no dihedral-angle violations $>5^\circ$. All structural representations were created with the program MOLMOL [32].

The β-turn (type III) comprising Thr[17], Ile[18], Glu[19], and Met[20] was defined by the distances between the C$^\alpha(i)$ and the C$^\alpha(i+3)$, which are in a range of 5.6 Å as described by *Rose et al.* [33]. The second evidence for a β-turn (type III) were the torsion angles $\phi(i+1)=-120^\circ$ and $\psi(i+1)=-30^\circ$ for Ile[18] and $\phi(i+2)=-30^\circ$ and $\psi(i+2)=-120^\circ$ for Glu[19]. No H-bond could be detected between the O′ of Thr[17] and the H^N of Met[20]. The coordinates of the final ten PLN (C41F) structures have been deposited with the *Brookhaven Protein Data Bank* under the PDB iD code 1FJP.

REFERENCES

[1] P. L. Pedersen, E. Carafoli, *Trends Biochem. Science* **1987**, *12*, 146.
[2] R. W. Tsien, *Adv. Cycl. Nucl. Res.* **1977**, *8*, 363.
[3] M. Tada, M. A. Kirchberger, D. I. Repke, A. M. Katz, *J. Biol. Chem.* **1974**, *249*, 6174.
[4] M. Tada, M. A. Kirchberger, A. M. Katz, *J. Biol. Chem*. **1975**, *250*, 2640.
[5] C. J. Lepeuch, J. Haiech, J. G. Demaille, *Biochemistry* **1979**, *18*, 5150.
[6] P. James, M. Inui, M. Tada, M. Chiesi, E. Carafoli, *Nature (London)* **1989**, *342*, 90.
[7] T. Toyofoku, K. Kurzydlowski, M. Tada, D. H. MacLennan, *J. Biol. Chem*. **1994**, *269*, 22929.
[8] Y. Kimura, K. Kurzydlowski, M. Tada, D. H. MacLennan, *J. Biol. Chem.* **1997**, *272*, 15061.
[9] M. Asashi, Y. Kimura, K. Kurzydlowski, M. Tada, D. H. MacLennan, *J. Biol. Chem.* **1999**, *274*, 32855.
[10] J. Fuji, K. Maruyama, M. Tada, D. H. MacLennan, *J. Biol. Chem.* **1989**, *264*, 12950.
[11] G. Chu, G. W. Dorn, W. Luo, J. M. Harrer, V. J. Kadambi, R. A. Walsh, E. G. Kranias, *Circ. Res.* **1997**, *81*, 485.
[12] P. Pollesello, A. Annila, M. Ovaska, *Biophys. J.* **1999**, *76*, 1784.
[13] B. A. Levine, V. B. Patchell, P. Sharma, Y. Gao, D. J. Bigelow, Q. Yao, S. Goh, J. Colyer, G. A. Drago, S. V. Perry, *Eur. J. Biochem*. **1999**, *264*, 905.
[14] I. V. Maslennikov, A. G. Sobol, J. Anagli, P. James, T. Vorherr, A. S. Arseniev, E. Carafoli, *Biochem. Biophys. Res. Commun*. **1995**, *217*, 1200.
[15] R. Gratias, H. Kessler, *J. Phys. Chem. B* **1998**, *102*, 2027.
[16] K. Wüthrich, 'NMR of Proteins and Nucleic Acids', Wiley, New York, 1986.
[17] J. J. Titman, J. Keeler, *J. Magn. Reson*. **1990**, *89*, 640.
[18] D. Wishart, B. Sykes, F. Richards, *J. Mol. Biol*. **1991**, *222*, 311.
[19] M. Nilges, S. I. O'Donoghue, *Prog. NMR Spectrosc.* **1998**, *32*, 107.
[20] A. T. Brünger, 'X-PLOR: A System for X-Ray Crystallography and NMR', Yale University Press, New Haven, CT, 1992.
[21] R. A. Laskowski, J. A. C. Rullmann, M. W. MacArthur, R. Kaptein, J. M. Thornton, *J. Biomol. NMR* **1996**, *8*, 477.
[22] J. M. Autry, L. R. Jones, *J. Biol. Chem*. **1997**, *272*, 15872.
[23] G. Hughes, J. M. East, A. G. Lee, *Biochem. J.* **1994**, *303*, 511.
[24] T. Vorherr, A. Wrzosek, M. Chiesi, E. Carafoli, *Protein Science* **1993**, *2*, 339.
[25] W. P. Aue, E. Bartholdy, R. R. Ernst, *J. Chem. Phys.* **1976**, *64*, 2229.
[26] L. Braunschweiler, R. R. Ernst, *J. Magn. Reson*. **1983**, *53*, 521.
[27] A. Kumar, R. R. Ernst, K. Wüthrich, *Biochem. Biophys. Res. Commun*. **1980**, *95*, 1.
[28] D. Marion, M. Ikura, R. Tschudin, A. Bax, *J. Magn. Reson*. **1989**, *85*, 393.
[29] M. Piotto, V. Saudek, V. Sklenar, *J. Biomol. NMR* **1992**, *2*, 661.
[30] C. M. Fletcher, D. N. Jones, R. Diamond, D. Neuhaus, *J. Biomol. NMR* **1996**, *8*, 292.
[31] A. Pardi, M. Billeter, K. Wüthrich, *J. Mol. Biol*. **1984**, *180*, 741.
[32] R. Koradi, M. Billeter, K. Wüthrich, *J. Mol. Graphics* **1996**, *14*, 51.
[33] G. D. Rose, L. M. Gierasch, J. A. Smith, *Adv. Protein Chem*. **1985**, *37*, 1.

Received May 18, 2000